Satellite imagery used in constructing emission maps for air quality modelling in the Dubai-Sharjah (UAE) region

D. S. Zachary[1] & B. Farooq[2]
[1] *Embry-Riddle Aeronautical University (Worldwide campus) and the Henri-Tudor Public Research Center of Luxembourg, (CRP -CRTE), Luxembourg*
[2] *Physics Department, American University of Sharjah, U.A.E.*

Abstract

Streamlined construction of emissions maps using satellite imagery (JPEG - RGB images) is discussed. A filter algorithm (MATLAB) is used to extract a road network which is subsequently used as an input to a "fast" (reduced-order) urban air shed model for the Dubai-Sharjah (UAE) region. Validation of the model is done using averaged air quality scenarios in an extended (one month) campaign, revealing that O_3 production is VOC limited in mid to late afternoon (peak ozone times). The modelled NO_x and O_3 concentrations are in rough agreement with the three measuring stations used in this study (two in the city center and one at the city periphery); high O_3 levels are predicted down-wind (desert-side) of the Dubai-Sharjah city centers in mid-afternoon.
Keywords: air quality, reduced-model, ozone, NO_x, VOC, optimization.

1 Introduction

The Dubai-Sharjah (UAE) metropolitan region, henceforth DS, covering approximately 15×60 km^2, represents one of the world's and fastest growing major metropolitan areas. The rapidly evolving transportation infrastructure has demanded that an efficient algorithm be developed which could be an alternative to the arduously constructed road networks using GIS traffic management software. The non-linear O_3 production from precursor gases NO_x and VOC is extremely CPU intensive and thus created the necessity for the fast ozone calculator TAPOM-

WIT Transactions on Ecology and the Environment, Vol 101, © 2007 WIT Press
www.witpress.com, ISSN 1743-3541 (on-line)
doi:10.2495/AIR070121

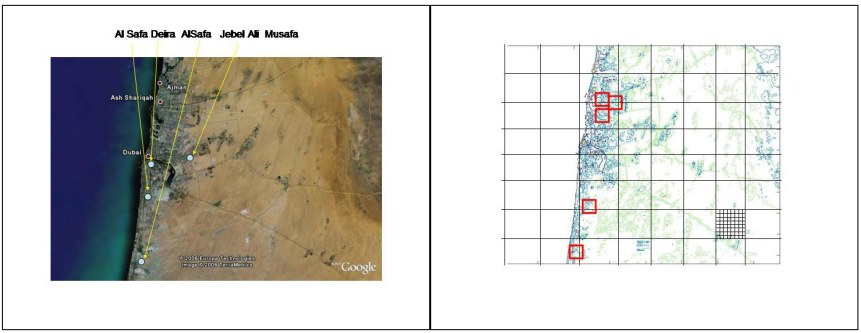

Figure 1: Satellite image (Google-Earth, public online software)) transformed to a colored bitmap mesoscale emissions image for the DS metropolitan region. The 30×30 km^2 and 500×500 m^2 (lower right example). The thick red boxed regions represent the industrial emissions area.

Lite, hereby referred to as TL. (An adaptation of a 3-D photochemical dispersion model TAPOM (Transport Pollution Model).)

The emissions input (primary road networks) are required as input to TL and this report focuses on the methodology used to construct this network using RGB (Red-Green-Blue JPEG satellite images) as input to TL. This study accompanies a parallel paper [1] that explores various air quality scenarios, including a worse case scenarios using this emissions network reported here. Figure (1) shows a Google-Earth [2] ©JPEG image of the mesoscale region, the domain is centered on Latitude $25°15'$ N, Longitude $55°16'$ E. The 24-hour air quality episodes uses time steps of 1 minute and 30×30 m^2 horizontal grid spacing (at ground level) and 200m vertical grid spacing.

We proceed with a description of the use of satellite imagery for the DS region and the methodology of the road network creation (Section 2) and we follow with results of air quality modelling for the one month campaign (Section 3) and conclude (Section 4).

2 Using satellite imagery to constructing an emissions network

The total amount of NO_x and VOC present in the DS urban air-shed region was calculated using a top-down approach. The initial concentrations of the two gases used for employing this method were obtained from the database of a global emissions inventory EDGAR [3] that has been constructed for each country through a joint venture by RIVM-MNP (Netherlands), TNO-MEP (Netherlands), JRC-IES, Ispra (Italy) and MPIC-AC, Mainz (Denmark). This extensive database includes concentrations of NO_x, methane (CH4), and Non-methane VOCs produced from a variety of broad categories at the national level in units of gigagrams for the year 2000.

Five major industrial areas in the DS region are also identified and all industrial emission are modelled as emanating from the red square regions of Figure 1. The total traffic and industry emissions in tons/yr. Data from 2005 estimate, is adjusted for 2007: 129'220, 76'865, 13'716, 8577 tons/year for traffic NO_x and VOC, industry NO_x and VOC respectively (Undergraduate Thesis, B. Farooq, 2004).

The current modeling initiative in the DS region was the construction of emissions geo-spatial distributions which are divided into two parts: emissions emanating from *traffic* and *industrial* sources. Most NO_x sources come from line sources (traffic) and VOC from area sources (e.g. gas stations) [4], suggesting that a model using an image of the region would mimic the distribution of these sources. The region's rapidity evolving traffic infrastructure called for an innovative way to model the emission line sources; thus a major development presented here is the construction of an emission network from traffic using satellite imagery and to a lesser extent, the modelling of industrial emissions. This initiative converted a digital satellite image (Figure 1), to a matrix map of the region, with resolution 30×30 m^2 (Figure 2). The O_3 concentrations calculated by TL are then compared to the actual measured concentrations at the locations of the monitoring stations in Dubai.

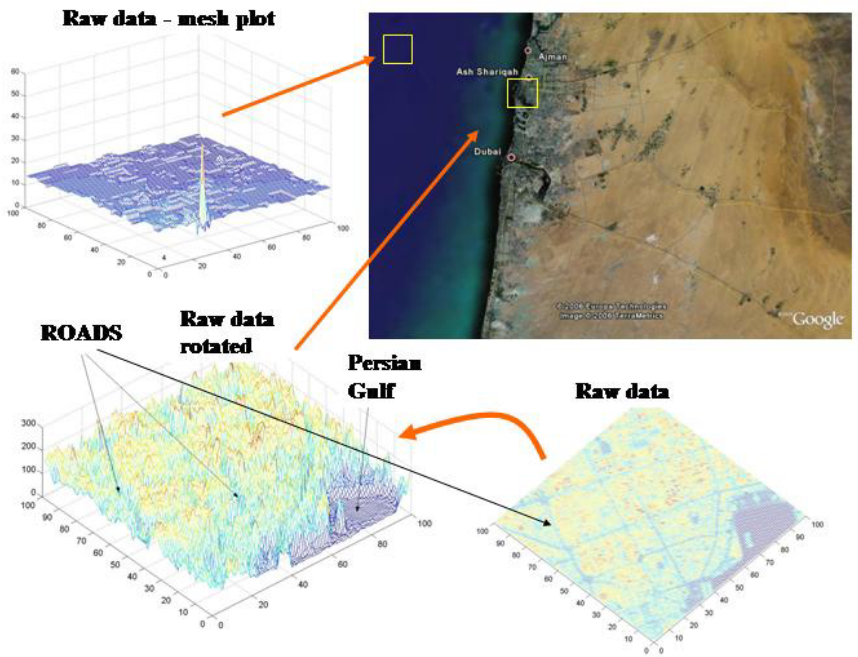

Figure 2: Examples of RGB [0,255] segmented bitmap transformed JPEG image of the DS region: (upper left) sea and (lower left) land. Also shown is the image rotated and viewed from above (lower right) [1].

A 1300×1000 pixel bitmap (RGB colorspace) of DS was created from a JPG formatted image. The traffic emission are treated using a simple algorithm, a MATLAB © command `imread`, used to extract the image (originally 30×30 km^2) to a digital format of resolution 30×30 m^2. The created images has assigned numbers ranging from [0,255] that represent the shades and colors of the original image. Roads were empirically identified as the RGB color code between ($50 <$ RGB < 80) and water or sea as RGB color code ($0 <$ RGB < 30), we refer to as SEA (Figure 3, lower left). A simple algorithm was used to distinguish roads from all other surface features. Defining the current grid in the image as $CG(x, y)$ in Cartesian coordinates, $x \in (1, 1300)$, $y \in (1, 1000)$ (grid or pixel space), the following conditions had to be satisfied in order that the grid was identified as road (RD) and not as a false "road" artifact (NRD), building, land or sea.

condition	action
$CG(x, y) \in RD$	CONDITION 1
$CG(x \pm 1, y) \in RD\ OR\ CG(x, y \pm 1) \in RD$	CONDITION 2
$CG(x \pm 1, y \pm 1) \in RD\ AND\ CG(x\mp, y \pm 1) \in RD$	CONDITION 3
$CG(x \pm 1, y) \notin SEA\ AND\ CG(x, y \pm 1) \notin SEA\ AND$	
$CG(x \pm 1, y \pm 1) \notin SEA\ AND\ CG(x\mp, y \pm 1) \notin SEA$	CONDITION 4
$CG(x \pm 2, y) \notin SEA\ AND\ CG(x, y \pm 2) \notin SEA\ AND$	
$CG(x \pm 2, y \pm 2) \notin SEA\ AND\ CG(x\mp, y \pm 2) \notin SEA$	CONDITION 5

The conditions are defined in the following way: Condition 1 - pixel is identified as road, Condition 2 - adjacent pixel on image axis is identified as road, Condition 3 - pixel on axis diagonal to image axis is identified as road, Conditions 4 and 5 - at least two pixels separate it from the SEA. If Conditions 1–5 are all satisfied, the pixel is accepted as "road" surface, otherwise it is either land or sea. The algorithm naturally identifies the width of the road and hence the type of road (with its accompanying typical traffic speeds). This algorithm was also shown to be an improvement over an earlier test explored in [1] which tested only the "on axis" grid points (Conditions 1 and 2 only) and did not contain the NRD algorithms (Conditions 4 and 5). The NRD test was a significant improvement as it helped to eliminate the false road identification due to the fall and rising slopes from sea to land in the RGB color change, clearly seen at pixels 35, 85, and 93 of Figure 3 (lower left).

An assigned road pixel, labelled $GC(x, y)^*$, must be further processed due to insufficient resolution of the JPEG picture; A resolution algorithm is therefore used to treat identified road pixels. A second treatment was applied to traffic emissions in order to take into account the lessening of traffic density away from either the Sharjah or Dubai city centers. The following weighting schemes were used,

$$f_S(x, y) = e^{-(x^2 - x_s^2)/\sigma_S^2} \cdot e^{-(y^2 - y_s^2)/\sigma_S^2} \tag{1}$$

$$f_D(x, y) = e^{-(x^2 - x_d^2)/\sigma_D^2} \cdot e^{-(y^2 - y_d^2)/\sigma_D^2} \tag{2}$$

$$CG^{**}(x, y) = CG^*(x, y) \cdot f_S(x, y) \cdot f_D(x, y) \tag{3}$$

where (x_d, y_d) represents the center grid of Dubai (Bur Dubai center, the Al-Maktoum bridge) and (x_s, y_s) represents center grid of Sharjah (Blue Souk center).

Daily emission scheduling is done in $60 \times 24 = 1440$ steps of one minute and weighted using a reasonable scheduling factor. The scheduling factor $f(t)$, is a "double-hump", $f(t) = m \cdot (t - t_o) + b_o$, increasing from midnight until morning (00:00–06:00), decreasing from morning until noon (06:00–12:00) and then repeating this pattern from 12:00 - 24:00, where $m_i = \pm 1.5/t_o$, $b_i =$

factor $f(t)$	time
$m_{night} \cdot (t - t_{night}) + b_{night}$	(00:00 - 06:00)
$m_{morn} \cdot (t - t_{morn}) + b_{morn}$	(06:00 - 12:00)
$m_{aftern} \cdot (t - t_{aftern}) + b_{aftern}$	(12:00 - 18:00),
$m_{even} \cdot (t - t_{even}) + b_{even}$	(18:00 - 24:00),

$(0.5, 2.0, -2.5, 5.0)$, $t_i =$ (0,06:00, 12:00, 18:00, 24:00) where $i \in$(night, morn, aftern, even) and $t_o = 6 \times 60$ (minutes). The combined resolution smearing and traffic weighting gives a dynamic emission map, per primary species, $E_i(t, x, y) = f(t) \cdot f_D(x, y) f_S(x, y) \cdot E_{o,i}(x, y)$, where $E_{o,i} = \int_{map} E_{o,i}(x, y) dxdy$.

3 Air quality scenarios and conclusions

The aggregated and non-speciated total VOC and NO_x are distributed using traffic network and the averaged O_3 and NO_x levels measured and simulated between the dates 11 September and 30 October 2006 are shown in Figure 5. No validation for VOC can currently be done in Dubai. Simulations were done using daily meteorology and a 24 hour spin-up time to bring the gas concentrations to acceptable levels before the actual simulation. The results of these comparison can be summarized in the following observations [1].

NO_x concentrations peak in the early morning hours, prior to 09:00, drop to a minimum in mid to late afternoons and again peak after 21:00. Partial quenching of NO_x is largely attributed to O_3 production and to a lesser part advection; between 15:00 and 18:00, NO_x levels typically drop to 10–20 ppb (at all stations) and are consistent with the increased O_3 production during this time.

O_3 concentrations peak in the late afternoon (measured) and the model predicts peaks at 12:00. Between 18:00 and 06:00, O_3 levels drop to near zero. Over advection, simplified meteorology, and the simplified NO_x and VOC scheduling in the model attributes to low levels at these times and also accounts for too early peaking of O_3. Model predictions show limited VOC available in late afternoons and contributes to low O_3 levels.

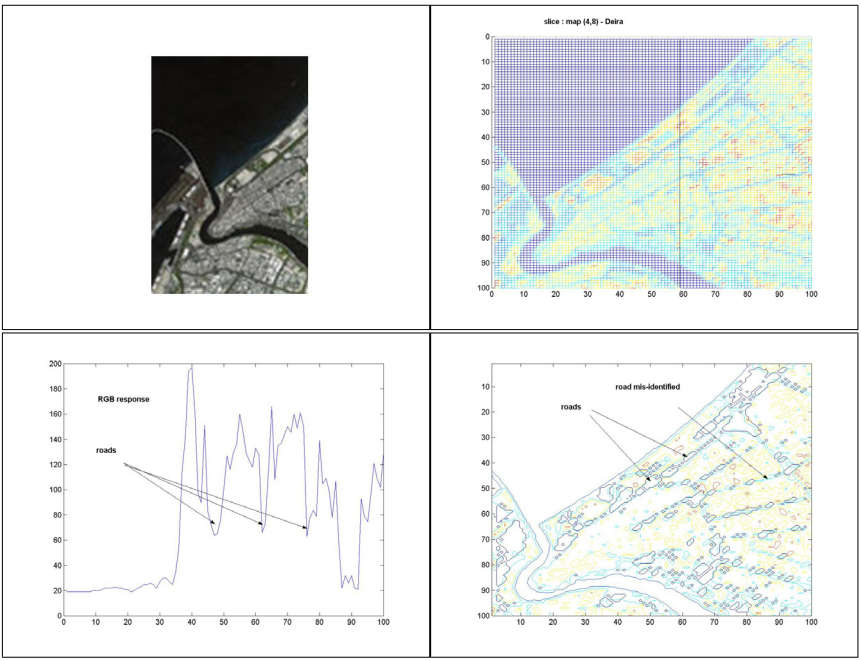

Figure 3: Deira (Dubai city center) satellite JPG image (upper left), RGB image showing image axis cut (upper right), RGB slice (lower left), filter contour plot satisfying Conditions 1–5 (lower right).

Trends in spatial evolution show the highest O_3 levels tend to be slightly downwind (desert side) of the highest road-density regions of DS (Dubia's Deira and creek-region). The high levels of ozone here indicate a need for measuring stations in regions of the air shed that are currently under-represented.

TL model was specifically designed for "averaged air quality scenarios" and is used in the integrated assessment framework of coupled models (metamodels). An example of averaged scenarios is shown in Table 1 where noontime O_3 and NO_x values are shown at the three measuring sites and compared to modeled values.

The speed of TL calculation is its strength but the "flip-side" is its weakness of accuracy, certainly at short time scales (less than one minute) and in a spatial micro view of the urban region (few 10s of meters). The inability for TL to consistently reproduce individual measurement stations is an indication of this weakness. Future improvements of the model's meteorology simulation will ameliorate this inaccuracy. (It should be noted that even the most accurate chemistry simulations and high resolution models have great difficulty in reproducing O_3 levels throughout a large urban air-shed at every point at all times.)

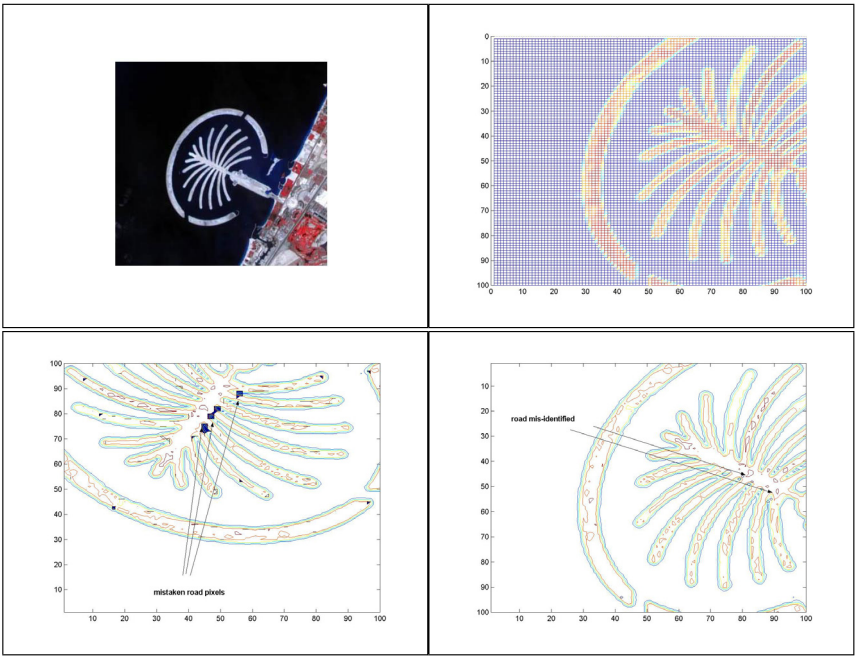

Figure 4: Palm satellite JPG image (upper left), RGB image (upper right), misidentified roads - black dots using Conditions 1 and 2 only (lower left), filter contour plot satisfying Conditions 1–5 (lower right).

4 Conclusions

TAPOM-Lite is a fast air quality calculator designed for determining trends in averaged meteorological episodes in integrated assessment work. The tool has been validated and simulations showing VOC limited O_3 production in the DS region; the lack of natural VOC sources partly explain this; O_3 peaks at midday in the simulation, approximately 3 hours earlier than measurements; simplifications in meteorology and emissions scheduling are accredited to this difference. We foresee a continued improvement on TL with the understanding that CPU costs be kept low so that the model remains viable in the optimization framework. Improvements will include a more accurate meteorology and NO_x and VOC aggregation schemes. A new application of this model is now underway for the city of Luxembourg.

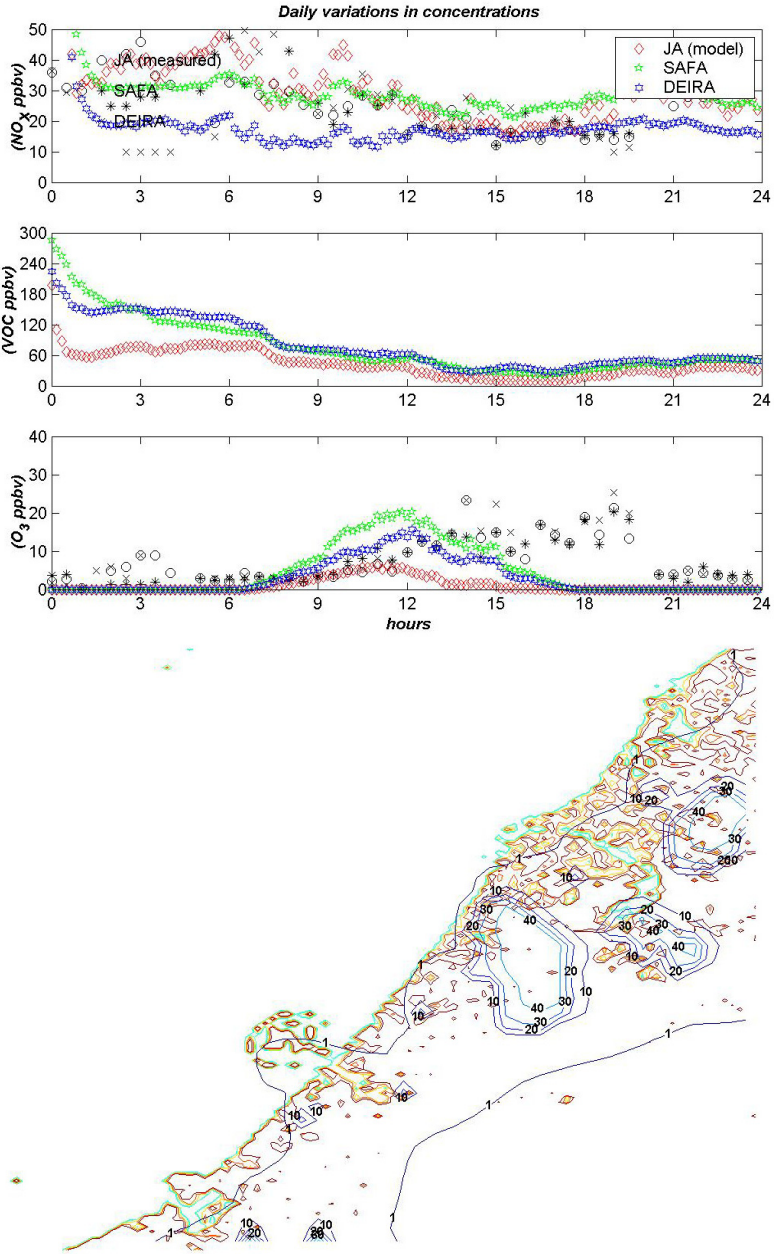

Figure 5: (a) Averaged daily variations of NO_x and O_3 (including simulated VOC) at three Dubai stations (Deira, Safa Park, and Jebel-Ali JA). Data taken from 11 September - 30 October 2006 campaign. (b) Contour plot of averaged O_3 levels at 12:00.

Table 1: Model/data comparison with measured stations on 11–15 September and averaged scenarios including extra data from 12–30 October 2006.

	Deira		Safa		Jebel Ali	
date	NO_x	O_3	NO_x	O_3	NO_x	O_3
11 Sept 06	21.1/17.7	14.9/8	33.4 /36.	24.2/4.5	34.7/26.	4.8 /10.5
12 Sept 06	15.4/12.	9.1/6	22.7 /37.	12.6/11.	20.0/23.	2.5 /6.
13 Sept 06	19.2/18.	20.1/18	30.4 /42.	25.9/7.	36.4/20.	6.5 /21.
14 Sept 06	9.2/17.	8.1/6	19.6 /18.	14.6/7.	19.2/15.	2.6 /7.
15 Sept 06	13.9/—	25.0/15	26.7/—	18.8/9.	30.6/—	4.1 /—
(*average*)	15.7/16.2	15.4/10.6	26.6/33.3	18.6/7.7	28.2/21.	4.1/11.1

Acknowledgements

Part of the work was completed at Physics Department, American University of Sharjah, U.A.E. and HEC, University of Geneva, Switzerland. We would like to thank the Dubai Municipality for their service in providing electronic data that was essential for the validation of this work. We would also like to thank Dr. Nidal Guessoum for his useful input in making this work complete.

References

[1] Zachary, D. & Farooq, B., Air quality scenarios in the Dubai-Sharjah metropolitan area using a reduced order air quality model and satellite imagery in constructing linear emission sources. Technical report, Embry-Riddle Aeronautical University and Henri Tudor Public Research Center and the American University of Sharjah (UAE), 2006.

[2] Google, Google earth online image, 2006. (public online software).

[3] Olivier, J., Bouwman, A.F., Berdowski, J.J.M., Veldt, C., Bloos, J.P.J., Visschedijk, A.J.H., Van der Maas, C.W.M. & Zandveld, P.Y.J., Edgar v2.0 by rivm/tno: Sectoral emission inventories of greenhouse gases for 1990 on a per country basis as well as on 1×1 degrees. *Environmental Science & Policy*, **2**, pp. 241264, 1999.

[4] Kim, C.H., Park, S.U. & Song, C.K., A simple semi-empirical photochemical model for the simulation of ozone concentration in the Seoul metropolian area in Korea. Atmospheric Environment, **39**, pp. 55975607, 2005.